geoconvention
Calgary • Canada • May 15-19 2017

The Role of Density in Elastic Full-waveform Inversion

Wenyong Pan[1], Yanhua Yuan[2], Frederik Simons[2], Kris Innanen[1]

1 Department of Geoscience, CREWES Project, University of Calgary

2 Department of Geoscience, Princeton University

Summary

Subsurface elastic properties are essentially important for reservoir characterizations. Reconstructing multiple physical parameters suffers from a series of difficulties including cycle-skipping and parameter crosstalk difficulties. Density structures are very important to characterize fluid reservoirs but remain to be poorly constrained, which may be caused by weak sensitivity to travel time and strong contaminations from velocity parameters. In this paper, we first give the scattering patterns of isotropic-elastic parameters in different parameterizations, which help understand the coupling effects between different physical parameters. In the numerical modeling section, we first give example illustrating the difficulty of recovering density. We then focus on studying the interparameter contaminations of isotropic-elastic parameters with different parameterizations.

Introduction

Full-waveform inversion techniques are considered to be promising for providing high resolution estimates of subsurface properties. However, because of the lack of low frequencies and inaccurate initial model, even just P-wave velocity is quite difficult to be recovered resulting from the high nonlinearity of the inverse problem. Researchers devote significant efforts to overcome the cycle-skipping problem (Pan et al., 2016b).

Incorporating elasticity into full-waveform inversion is becoming very necessary, because subsurface media is more appropriate to be described by elasticity and the elastic properties are very important for reservoir characterization (Yanhua and Simons, 2014; Yanhua et al., 2015). However, recovering multiple elastic parameters is much more challenging. The cycle-skipping problem becomes more serious. Furthermore, the coupling effects between different physical parameters result in parameter crosstalk artifacts, which increases the nonlinearity and uncertainties of inverse problem significantly (Pan et al., 2016). Knowledge of subsurface density heterogeneities is essentially important for fluid reservoir characterization. However, the density structures are still poorly constrained in FWI, which may be caused by the strong interparameter contaminations from velocity parameters and the week sensitivity of travel time to density variations.

To understand the interparameter coupling effect, we formulate the correlation and scattering coefficients of isotropic-elastic parameters for modulus, velocity, and impedance parameterizations following the framework of scattering potentials developed by Stolt and Weglein (2012). In velocity parameterization, the scattered wave due to density perturbation propagates backward. Examining P-P scattering patterns informs us that it will be difficult to distinguish P-wave velocity diffractor and density diffractor at near offset. In impedance parameterization, the scattered wave due to density perturbation propagates forward meaning that retrieving density with reflection survey will be difficult for impedance parameterization.

However, we find that the interparameter contaminations are so complex that the scattering patterns may not be enough to explain them completely. Hessian operator represents the second derivative of the misfit function and provides more complete and direct measurements of spatial and interparameter

tradeoffs. Elements in off-diagonal blocks measure the correlations of different physical parameters (Pan et al., 2015; Pan et al., 2016; Pan et al., 2017). For large-scale inverse problems, it is unaffordable to construct multiparameter Hessian explicitly. In this paper, we calculate multiparmaeter point spread functions (MPSFs), which are proportional to multiparameter Hessian columns, to evaluate the interparameter tradeoffs.

Full-waveform Inversion: Theory

Full-waveform inversion (FWI) seeks to estimate the subsurface (an) elastic and anisotropic properties by iteratively minimizing the differences between seismic observations and synthetic data. The misfit function is formulated as L-2 norm (Yuan et al., 14; Pan et al., 2014b):

$$\Phi(\mathrm{m}) = \frac{1}{2}\sum_{s=1}^{S}\sum_{r=1}^{R}\left\|\Delta \mathrm{d}(x_s, x_r, t; \mathrm{m})\right\| dt, \tag{1}$$

where $\Delta \mathrm{d}(x_s, x_r, t; \mathrm{m})$ is the data residual. In order to solve the inverse problem, the model is always updated iteratively. Within the Newton optimization framework, the search direction can be obtained by solving the Newton linear system: $\mathrm{H}_k \Delta \mathrm{m}_k = -\nabla_{\mathrm{m}} \Phi_k$, where $\nabla_{\mathrm{m}} \Phi_k$ and H_k are gradient and Hessian respectively. Gradient of the misfit function corresponding to Bulk modulus κ, shear modulus μ and density ρ can be expressed as:

$$\begin{aligned}\nabla_{\mathrm{m}}\Phi(\mathrm{m}) = -\sum_{s=1}^{S}\sum_{r=1}^{R}\int_0^T\int_{\Omega(\mathrm{x})}\int_0^t \Big[\Delta\rho(\mathrm{x})G_{ni}(\mathrm{x},\mathrm{x}_r,t-t')\partial_t^2 u_i(\mathrm{x},\mathrm{x}_s,t') + \left(\Delta\kappa(\mathrm{x}) - \frac{2}{3}\Delta\mu(\mathrm{x})\right)\delta_{ij}\delta_{kl}\delta_j G_{ni}(\mathrm{x},\mathrm{x}_r,t-t')\partial_k u_l(\mathrm{x},\mathrm{x}_s,t') \\ + \Delta\mu(\mathrm{x})\left(\delta_{ik}\delta_{jl}+\delta_{jk}\delta_{il}\right)\delta_j G_{ni}(\mathrm{x},\mathrm{x}_r,t-t')\partial_k u_i(\mathrm{x},\mathrm{x}_s,t')\Big]\Delta\mathrm{d}(x_s,x_r,t;\mathrm{m})dt'd\mathrm{x}dt,\end{aligned} \tag{2}$$

where G_{ni} is the Green's function. Explicit expressions of the sensitivity kernels for bulk modulus κ, shear modulus μ and density ρ are given by:

$$\begin{aligned}K_\kappa &= -\sum_{s=1}^{S}\sum_{r=1}^{R}\int_0^T\int_{\Omega(\mathrm{x})}\kappa(\mathrm{x})\left[\nabla\cdot\mathrm{u}^*(\mathrm{x}_r,\mathrm{x},T\text{-}t)\right]\left[\nabla\cdot\mathrm{u}(\mathrm{x},\mathrm{x}_s,t)\right]dtd\mathrm{x}, \quad K_\mu = -\sum_{s=1}^{S}\sum_{r=1}^{R}\int_0^T\int_{\Omega(\mathrm{x})}2\mu(\mathrm{x})\mathrm{D}^*(\mathrm{x}_r,\mathrm{x},T\text{-}t):\mathrm{D}(\mathrm{x},\mathrm{x}_s,t)dtd\mathrm{x}, \\ K_\rho &= -\sum_{s=1}^{S}\sum_{r=1}^{R}\int_0^T\int_{\Omega(\mathrm{x})}\rho(\mathrm{x})\mathrm{u}^*(\mathrm{x}_r,\mathrm{x},T\text{-}t)\partial_t^2\mathrm{u}(\mathrm{x},\mathrm{x}_s,t)dtd\mathrm{x},\end{aligned} \tag{3}$$

where D is the traceless strain deviator. The sensitivity kernels for P-wave velocity α, shear-wave velocity β and density ρ' are given by:

$$K_\alpha = 2\left(1+\frac{4\mu}{3\kappa}\right)K_\kappa, K_\beta = 2\left(K_\mu - \frac{4\mu}{3\kappa}\right)K_\kappa, K_{\rho'} = K_\kappa + K_\mu + K_\rho. \tag{4}$$

According the chain rule, we can obtain the sensitivity kernels for P-wave impedance IP, S-wave impedance IS, and density ρ'':

$$K_{IP} = \frac{1}{\rho''}K_\alpha, K_{IS} = \frac{1}{\rho''}K_\beta, K_{\rho''} = K_{\rho'} - \frac{\alpha}{\rho''}K_\alpha - \frac{\beta}{\rho''}K_\beta. \tag{5}$$

Scattering and Correlation Coefficients of Isotropic-elastic Parameters

Scattering coefficients corresponding to modulus, velocity and impedance parameterizations in isotropic-elastic media can be formulated following the framework of scattering potentials developed by Stolt and Weglein (2012). An incident plane wave is scattered due to a local heterogeneity embedded in an isotropic-elastic background. Scattering potential is defined as the difference between the wave operators in the perturbed and unperturbed medium and describes the wave scattering due to model perturbations. For isotropic-elastic media, the scattering potential in displacement space can be expressed in terms of wavenumers:

$$V_{ij} = -\kappa\vec{\mathbf{k}}_i a_\kappa \vec{\mathbf{k}}_j - \frac{4}{3}\mu\vec{\mathbf{k}}_i a_\mu \vec{\mathbf{k}}_j + \rho\delta_{ij}\omega^2 a_\rho + \mu\delta_{ij}\sum_q \vec{\mathbf{k}}_q a_\mu \vec{\mathbf{k}}_q + 2\mu\vec{\mathbf{k}}_i a_\mu \vec{\mathbf{k}}_j + \mu\vec{\mathbf{k}}_j a_\mu \vec{\mathbf{k}}_i, \tag{6}$$

where i and j take on the values of x, y, z, a_q indicates the relation model perturbation of model parameter q. $\overleftarrow{\mathbf{k}}$ and $\vec{\mathbf{k}}$ represent wavenumber vectors of indicate and scattered waves. Applying curl and divergence operations decomposes the scattering potentials into P and S wave components. With the help of rotation matrix, SV and SH wave modes can be separated (Stolt and Weglein, 2012). The resulting scattering potential operator is an 3X3 matrix, with diagonal elements describe scattering that preserves wave type and off-diagonal elements describe scattering that convert wave type. We derive the scattering potentials of isotropic-elastic parameters with different parameterizations, as illustrated in Figure 1. The correlations coefficients are defined as the inner product of the scattering coefficients.

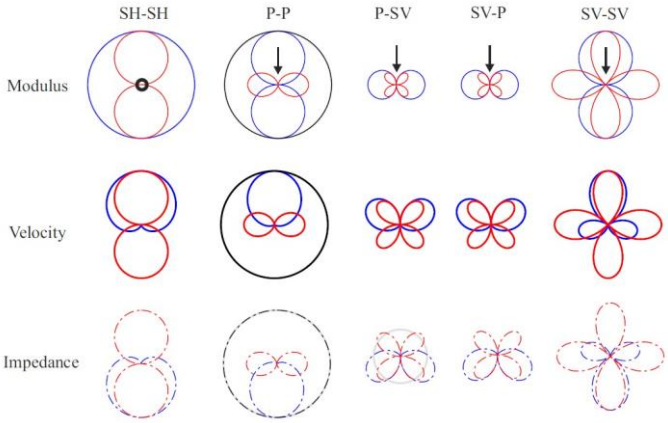

Figure 1. Scattering patterns of isotropic-elastic parameters for modulus, velocity and impedance parameterizations.

As we can see, in velocity parameterization, the scattered wave due to density perturbation propagates backward. Examining P-P scattering patterns informs us that it will be difficult to distinguish P-wave velocity diffractor and density diffractor at near offset. In impedance parameterization, the scattered wave due to density perturbation propagates forward meaning that retrieving density with reflection survey will be difficult for impedance parameterization.

Numerical Examples

From Figure 2 and Figure 3, we see that the P-wave and S-wave velocity are well reconstructed but density structures are poorly recovered, which may be caused the parameter contaminations from S-wave velocity (Pan et al., 2017b).

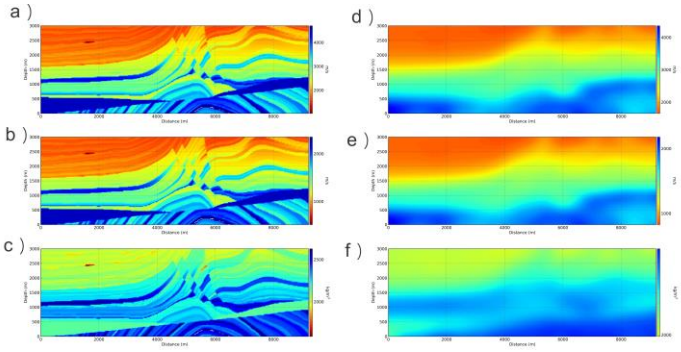

Figure 2. Panels (a-c) show the true P-wave velocity, S-wave velocity and density models. Panels (d-f) show the corresponding initial models.

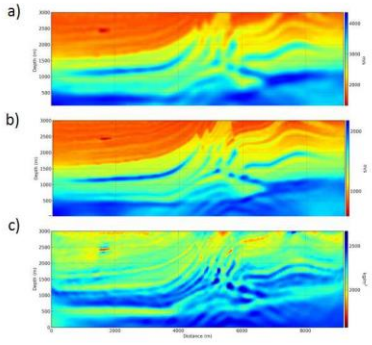

Figure 3. Panels (a-c) show the inverted P-wave velocity, S-wave velocity and density models.

To quantity the inter parameter contaminations of the isotropic-elastic parameters in different parameterizations, we calculate the multiparameter point spread functions. In Pan et al., (2017b), we show the MPSFs in velocity parameterization. In Figure 4, we show the MPSFs with modulus and impedance parameterizations respectively. We observe that in modulus parameterization, density produces strong contaminations in both bulk modulus and shear modulus. For impedance parameterization, S-wave impedance perturbation results in strong artifacts in P-wave impedance and density.

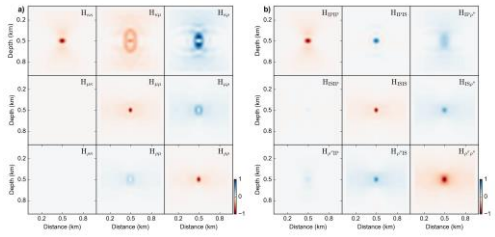

Figure 4. (a) show the multiparameter point spread functions (MPSFs) for isotropic-elastic parameters in modulus parameterization; (b) show the multiparameter point spread functions (MPSFs) for isotropic-elastic parameters in impedance parameterization.

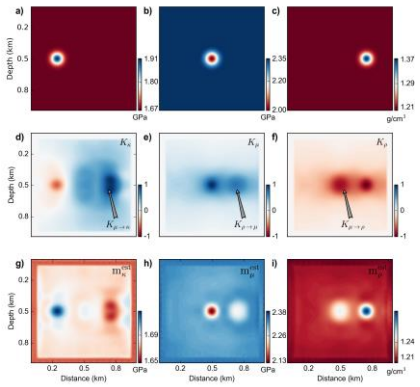

Figure 5. Panels (a-i) show the true bulk modulus, shear modulus and density models, sensitivity kernels and the corresponding inverted models.

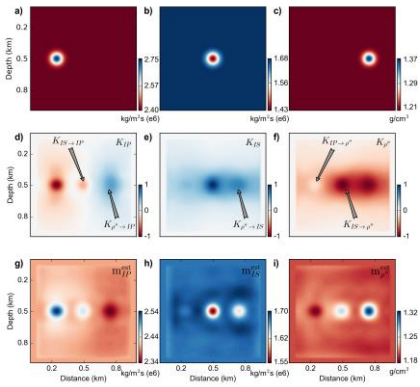

Figure 6. Panels (a-i) show the true P-wave impedance, S-wave imepdance and density models, sensitivity kernels and the corresponding inverted models.

To verify our predictions, we carry out inversion experiments with two Gaussian anomaly examples with a perfect acquisition geometry. Figure 5 show the true modulus and density models, sensitivity kernels and the corresponding inverted models. Figure 6 show the true impedance and density models, sensitivity kernels and the corresponding inverted models. We observe that impedance parameterization suffers strong parameter artifacts than modulus parameterization.

Conclusions

In this paper, we explain the difficulty of recovering density in elastic FWI. The correlation and scattering coefficients of isotropic-elastic parameters with modulus, velocity and impedance parameterizations are given. The interparameter tradeoffs with different parameterizations are studied.

Acknowledgements

This research was supported by the Consortium for Research in Elastic Wave Exploration Seismology (CREWES) and National Science and Engineering Research Council of Canada (NSERC, CRDPJ 461179-13). Wenyong Pan is also supported by SEG/Chevron scholarship and Eyes High International Doctoral Scholarship.

References

Pan, W., K. A. Innanen, and G. F. Margrave, 2014a, A comparison of different scaling methods for least-squares migration/inversion: EAGE Expanded Abstracts, We G103 14.

Pan, W., G. F. Margrave, and K. A. Innanen, 2014b, Iterative modeling migration and inversion (IMMI): Combining full waveform inversion with standard inversion methodology: SEG Technical Program Expanded Abstracts, 938-943.

Pan, W., K. A. Innanen, G. F. Margrave, and D. Cao, 2015, Efficient pseudo-Gauss-Newton full-waveform inversion in the t-p domain: Geophysics, 80, no. 5, R225-R14.

Pan, W., K. A. Innanen, G. F. Margrave, M. C. Fehler, X. Fang, and J. Li, 2016, Estimation of elastic constants for HTI media using Gauss-Newton and full-Newton multiparameter full-waveform inversion: Geophysics, 81 (5), R275-R291.

Pan, W., K. A. Innanen, and W. Liao, 2017, Accelerating Hessian-free Gauss-Newton full-waveform inversion via *l*-BFGS preconditioned conjugate-gradient algorithm: Geophysics, 82 (2), 1-16.

Pan, W., K. A. Innanen, Y. Yuan, and F. Simons, 2017b, Quantifying parameter trade-off in elastic full-waveform inversion via multi-parameter Hessian probing, GeoConvention.

Pan, W., K. A. Innanen, G. M, and S. Keating, 2016b, Mitigate Cycle-skipping for Full-waveform Inversion by Band-limited Impedance Inversion and POCS, GeoConvention.

Yanhua, Y. O. and F. J. Simons, 2014, Multiscale adjoint waveform difference tomography using wavelets: Geophysics, 79, no. 3, WA79–WA95.

Yanhua, Y. O., F. J. Simons, and E. Bozdaˇg, 2015, Multiscale adjoint waveform tomography for surface and body waves: Geophysics, 80, no. 5, R281–R302.

Stolt, R. H. and A. B. Weglein, 2012, Seismic imaging and inversion: Application of linear inverse theory: Cambriage University Press.